Contents lists available at ScienceDirect

Physics Letters B

PHYSICS LETTERS B

New short-lived isotope ^{223}Np and the absence of the $Z = 92$ subshell closure near $N = 126$

CrossMark

M.D. Sun [a,b,c], Z. Liu [a,*], T.H. Huang [a], W.Q. Zhang [a], J.G. Wang [a], X.Y. Liu [a,b], B. Ding [a], Z.G. Gan [a], L. Ma [a], H.B. Yang [a], Z.Y. Zhang [a], L. Yu [a], J. Jiang [a,b], K.L. Wang [a,b], Y.S. Wang [a], M.L. Liu [a], Z.H. Li [d], J. Li [d], X. Wang [d], H.Y. Lu [a,b], C.J. Lin [e], L.J. Sun [e], N.R. Ma [e], C.X. Yuan [f], W. Zuo [a], H.S. Xu [a], X.H. Zhou [a], G.Q. Xiao [a], C. Qi [g], F.S. Zhang [h,i]

[a] *Institute of Modern Physics, Chinese Academy of Sciences, Lanzhou 730000, China*
[b] *University of Chinese Academy of Sciences, Beijing 100049, China*
[c] *Lanzhou University, Lanzhou 730000, China*
[d] *State Key Laboratory of Nuclear Physics and Technology, School of Physics, Peking University, Beijing 100871, China*
[e] *China Institute of Atomic Energy, P.O. Box 275(10), Beijing 102413, China*
[f] *Sino-French Institute of Nuclear Engineering and Technology, Sun Yat-Sen University, Zhuhai, 519082, Guangdong, China*
[g] *KTH Royal Institute of Technology, Albanova University Center, SE-10691, Stockholm, Sweden*
[h] *Key Laboratory of Beam Technology and Material Modification of Ministry of Education, College of Nuclear Science and Technology, Beijing Normal University, Beijing 100875, China*
[i] *Beijing Radiation Center, Beijing 100875, China*

ARTICLE INFO

ABSTRACT

The $N = 130$ short-lived isotope ^{223}Np was produced as evaporation residue (ER) in the fusion reaction ^{40}Ar + ^{187}Re at the gas-filled recoil separator Spectrometer for Heavy Atom and Nuclear Structure (SHANS). It was identified through temporal and spatial correlations with α decays of ^{215}Ac and/or ^{211}Fr, the third and fourth members of the α-decay chain starting from ^{223}Np. The pileup signals of ER(^{223}Np)–α(^{223}Np)–α(^{219}Pa) were resolved by using the digital pulse processing technique. An α decay with half-life of $T_{1/2} = 2.15(^{100}_{52})$ µs and energy of $E_\alpha = 9477(44)$ keV was attributed to ^{223}Np. Spin and parity of $9/2^-$ were tentatively proposed for the ground state of ^{223}Np by combining the reduced α-decay width and large-scale shell-model calculations. This assignment together with the proton separation energy disprove the existence of a $Z = 92$ subshell closure.

© 2017 The Author(s). Published by Elsevier B.V. This is an open access article under the CC BY license (http://creativecommons.org/licenses/by/4.0/). Funded by SCOAP^3.

1. Introduction

The evolution of proton shell structure beyond ^{208}Pb is of decisive importance for the shell stabilization of superheavy elements. The existence of a subshell or even shell gap at $Z = 92$ between the proton $h_{9/2}$ and $f_{7/2}$ orbitals has been a topic of intense theoretical debate. A substantial $Z = 92$ shell gap is predicted in many relativistic mean-field calculations like an early work for heavy elements [1], in most of the covariant density functionals (CDFs) [2,3] and also in some non-relativistic models [4].

Macroscopic–microscopic calculations [5] predicted a subshell gap at $Z = 92$. This is at variance with large-scale shell-model calculations [6], which show no sign of a shell gap at $Z = 92$ for $N = 126$ isotones and are in overall agreement with spectroscopic data on these isotones up to U [6–10].

The spurious shell closures of $Z = 92$ and others can be cured in the upgraded CDF model [11] by including ρ-tensor Fock terms, restoring the pseudo-spin symmetry which qualitatively represents the balance of nuclear forces [11–13]. However, the very recent experimentally observed sudden decrease of the reduced α-decay width at $Z = 92$ along the $N = 130$ isotonic chain (see Fig. 5a in [14]) cannot exclude the possibility of a subshell closure at $Z = 92$ for $N > 126$. Further studies of isotopes beyond U in this region may shed light on the proton shell structure around

$Z = 92$. The proton separation energy, ground-state spin and parity of odd-Z isotopes beyond U, e.g. Np isotopes ($Z = 93$), could help clarify the absence/presence of the $Z = 92$ subshell closure. Such experimental verification is necessary and valuable for testing the nuclear structure models and understanding the nature of nuclear forces as well [11–13].

For isotopes of elements above lead and far off the β-stability line, α decay prevails as the major radioactive decay mode and α spectroscopy is an indispensable tool to investigate the low-energy structure of heavy neutron-deficient nuclei. In the classical picture, α decay occurs through the preformation of an α particle in the nucleus and its subsequent tunneling through Coulomb and centrifugal barriers [15,16]. Above shell closure, the preformation probability of α particle and the decay energy Q_α increase simultaneously, therefore the most enhanced α decays take place above doubly magic nucleus such as ^{208}Pb and ^{100}Sn [17,18].

All over the chart of nuclides, the region to the "north-east" of ^{208}Pb, with $Z \geq 84$ and $N = 128$–130, hosts the shortest-lived α radioactivities, with half-lives in the range of nanoseconds to microseconds. So far the shortest-lived α emitter known with directly measured half-life is ^{219}Pa ($T_{1/2} = 53$ ns) [19] with $N = 128$. Synthesis and detection of neutron-deficient isotopes above thorium in this region are challenging due to their low production cross sections and short half-lives. With increasing atomic number Z, the fission probability of the compound nucleus increases rapidly and the evaporation of protons and α particles is by far dominant over neutron evaporation [20]. Progress in this region has been very slow in the last three decades, the frontier in this region was only pushed forwards from Pa to U [14]. For the $N = 130$ isotones experimental data are available up to ^{222}U. Recently the semi-magic ^{219}Np ($N = 126$) was reported in [21] as the daughter of ^{223}Am, but the assignments of these two isotopes are in doubt because the half-life of ^{223}Am is expected much shorter while that of ^{219}Np much longer than claimed in [21]. The most neutron-deficient neptunium isotope ^{225}Np was discovered over 20 years ago [22].

In the present letter, we report on the first observation of the short-lived $N = 130$ neptunium isotope ^{223}Np. As its daughter nucleus ^{219}Pa is extremely short-lived, the α-decay signals of ^{223}Np and ^{219}Pa will pile up in the implantation detector, and even with the ^{223}Np implant signal if the half-life of ^{223}Np is in the range of microseconds. With conventional analog electronics, the shortest half-lives accessible are around tens of μs, it is extremely difficult or impossible to resolve these pileup signals in either energy or time. In recent years, digital pulse processing has been successfully applied to resolve such pileup events in the charged particle spectroscopy of short-lived nuclei [14,18,23].

2. Experiment and results

The isotope ^{223}Np was produced in the ^{187}Re(^{40}Ar, 4n) reaction channel with isotopically enriched (98.6%) ^{187}Re targets. The ^{40}Ar beam was accelerated to 188 MeV by the Sector-Focusing Cyclotron (SFC) of the Heavy Ion Research Facility in Lanzhou (HIRFL). The beam intensity on target, monitored via Faraday Cups upstream and downstream of the target chamber, was around 320 pnA in average during the entire experiment of 110 hours, with an uncertainty of up to a factor of 2. The targets were 460 μg/cm² thick, sputtered on carbon foils of thickness 80 μg/cm², with carbon foils facing the beam. After the experiment, target thicknesses were measured to be basically the same as before the experiment within a precision of ∼15%. In the center of the target, the excitation energy of the compound nucleus ^{227}Np is estimated to be 44 MeV, close to that expected for the maximum cross-section for ^{223}Np by the HIVAP code [24], with other main reaction channels

being ^{223}U(p3n evaporation channel), ^{220}Pa(α3n evaporation channel) and ^{220}Th(αp2n evaporation channel).

Evaporation residues were separated from the primary beam by the recoil separator SHANS [25] filled with ∼0.6 mbar helium gas and implanted into a 300-μm double-sided silicon strip detector (DSSSD). The average charge state, q, of the evaporation residues was simulated to be $q = 6.9$ [26]. For optimum transmission, the magnetic rigidity of SHANS was set to $B\rho = 1.785$ Tm. The DSSSD had 48 horizontal and 128 vertical strips of 1 mm width, forming a total of 6144 pixels. A multiwire proportional chamber (MWPC) was mounted in front of the DSSSD detector and was used to distinguish between implantation and decay events. To minimize the interference from scattered light ions in the DSSSD, three Si detectors of 50 mm × 50 mm size and 300 μm thick were placed side by side behind the DSSSD detector and used as veto detectors. Typical MWPC and DSSSD implantation detector rates were less than 100/s during beam-on periods, indicating a very good primary beam and transfer background suppression performance of SHANS.

In this experiment, very short-lived nuclei with $N = 128$–130 were produced either as ERs or as decay products of ERs. In order to resolve pileup signals, a data acquisition system based on fast digital pulse processing (DPP) was used. Signals from all the preamplifiers of the DSSSD strips, MWPC and veto detectors were digitized directly by using the 14-bit, 100-MS/s fADCs from CAEN S.p.A [27]. The digitizers allow for dead-time free acquisition, and all the channels are able to generate triggers independently. The timing is based on a so-called RC-CR² filter. In analogy with the constant-fraction discrimination, the RC-CR² signal is bipolar and its zero crossing corresponds to the trigger time-stamp. The preamplifier signals and RC-CR² signals were sampled simultaneously at the same frequency of 20 ns a sampling point and waveforms of 15 μs length were recorded for offline analysis.

Energy calibrations were performed with ^{175}Lu, ^{186}W and ^{187}Re targets at the same beam energy, covering a range of 6–19 MeV, specifically 6.3–9.4 MeV for single α energy and up to 19 MeV for double α sum energy. For non-pileup traces of long-lived α radioactivities, a trapezoidal filter with rising time 5 μs and flat top 3 μs was used to extract the full pulse height [28]. The energy resolution (FWHM) obtained with all vertical (horizontal) strips summed up is 22 (30) keV at α-particle energy of ∼7000 keV.

For pileup events, depending on the time difference ΔT between the overlapping signals, the energies of individual signals were extracted using different algorithms. For overlapping signals with $\Delta T = 0.5$–15 μs, a trapezoidal filter with rising time 200 ns and flat top 200 ns was used. For signals with $\Delta T = 200$–500 ns, the pulse-height of individual signal was obtained from the difference between the average of about six data points in the plateau area after the leading edge and that before the leading edge (average difference algorithm). The energy resolution of vertical strips for α decays recorded in double/multiple pulse traces with ΔT down to ∼0.5 μs and ∼0.2 μs are around 55 keV and 70 keV, respectively. In the interval $\Delta T = 100$–200 ns, the average difference algorithm was applied but with smaller number of data points, the energy resolution obtained is around 140 keV. It is worth noting that this is the shortest time difference between two overlapping pulses which have been analyzed in α/p spectroscopy, thanks to the very fast rising times of the signals from the DSSSD preamplifiers which are typically 40–60 ns in the present work. For even shorter time difference, $\Delta T < 100$ ns, the boundary between the two α pulses is difficult/impossible to determine. In some of such cases, the individual α energy may be extracted using the pulse height of each α, but the results will be rather arbitrary and unreliable.

For α pileup signals with $\Delta T < 200$ ns, where the two α signals are difficult/impossible to be separated, the sum am-
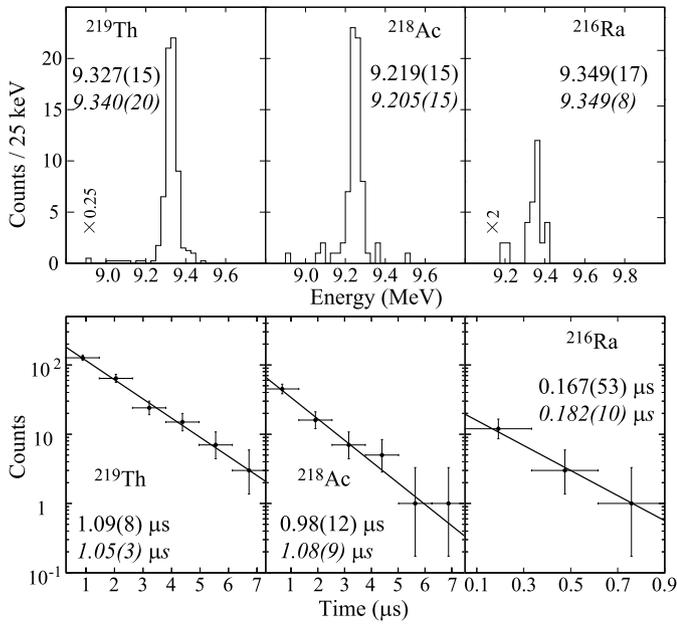
Fig. 1. The α energies, half-lives of ^{219}Th, ^{218}Ac and ^{216}Ra obtained from the present digital signal waveform analysis. The α energy and half-life values in italics below our results are from literature [29].

Fig. 2. Examples of multiple pulse traces in which ^{223}Np implant and subsequent α decays of ^{223}Np and ^{219}Pa were registered. In the middle and lower panels, the very closely spaced α-decay signals are zoomed in the inset. (Color online)

plitude was extracted using the average difference algorithm. The pile-up pulses of $\alpha(^{221}$Pa)–$\alpha(^{217}$Ac) ($T_{1/2} = 69$ ns) [29] and $\alpha(^{220}$Th)–$\alpha(^{216}$Ra) ($T_{1/2} = 182$ ns) [29], the sum energies of which are 18725 keV and 18139 keV [29], respectively, were used for the calibration at the high energy end. Though the statistics was low, the energy resolution of vertical strips obtained for these two sum energies is less than 90 keV.

Thus depending on the time difference ΔT, the standard deviation σ of single α-energy is 60, 30, 23 and 9 keV for $\Delta T =$ 100–200 ns, 200–500 ns, 0.5–15 μs and $\Delta T > 15$ μs, respectively. For $\Delta T < 100$ ns, only the sum energy can be extracted reliably and the standard deviation is taken as 40 keV. The calibration errors, i.e., the differences between the calibration values and the literature values, are less than 15 keV in the energy range of 6–19 MeV. In the present work, the systematic energy uncertainty was taken as 15 keV and the overall energy uncertainties were calculated as the quadrature of the statistical and systematic errors.

The $N = 129$ isotones ^{219}Th (ER) and ^{218}Ac (daughter of ^{222}Pa implant) have half-lives of around 1 μs, while the $N = 128$ isotone ^{216}Ra (daughter of ^{220}Th implant) has a half-life of 0.18 μs, making them suitable benchmarks for ER–α_1 or α_1–α_2 pileup trace analysis. The resolved α energy spectra and the decay curves for ^{219}Th, ^{218}Ac and ^{216}Ra are shown in Fig. 1. The α energies and half-lives measured in the present work are in good agreement with the literature values [29].

In order to identify decay chains belonging to ^{223}Np, all digital traces correlated to the subsequent α decay of ^{215}Ac ($E_\alpha = 7600(4)$ keV, $T_{1/2} = 0.17(1)$ s) [29] and/or ^{211}Fr ($E_\alpha = 6537(4)$ keV, $T_{1/2} = 3.10(2)$ min) [29], which are the third and fourth members of the α-decay chain originating from ^{223}Np, were checked event by event for the presence of multiple pulses. Ten multiple traces, all of which are triple pulse traces ER–α_1–α_2, were unambiguously attributed to the implantation of ^{223}Np followed by α decays of ^{223}Np and ^{219}Pa. The decay chains corresponding to these traces are listed in Table 1. As examples, the traces corresponding to events 1, 4 and 6 are plotted in Fig. 2.

The α sum energies of ^{223}Np and ^{219}Pa in five (events 1–5) of the ten decay chains are very close (within 50 keV) and much larger than the values in the rest, implying that only one α
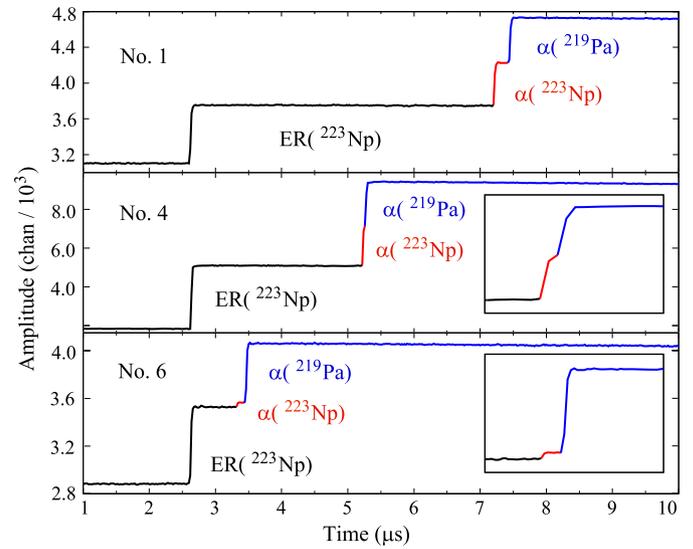
line was observed in ^{223}Np. In event 1, the full α energies of both ^{223}Np and ^{219}Pa can be extracted. In event 6, the full α energy of ^{219}Pa can be obtained while only part of the ^{223}Np α energy was registered. In decay chains 2–5, only the full sum energy of the α particles from ^{223}Np and ^{219}Pa can be deduced as individual α energies can not be extracted reliably due to too short time differences. In decay chains 7–10, at least one of the two α particles deposited partial energy or the time differences between the two overlapping α signals are too short.

From events 1–5, the full sum energy of α particles from ^{223}Np and ^{219}Pa is extracted to be 19453(23) keV. The error was calculated using a systematic uncertainty of 15 keV and standard deviation of 40 keV for events 1–5. From events 1 and 6, the full α energy of ^{219}Pa is obtained as 9976(37) keV, in agreement with the previous value of 9900(50) keV [19] within the error bar. In [19] the ERs were stopped in a catcher foil behind the target and α particles emitted from the stopper were detected with an ionization chamber, the energy resolution of which was poor (FWHM ~ 100 keV). The implantation-decay correlation measurement was not possible there, so the decay chain of ^{219}Pa was established for the first time here. The α energy of ^{223}Np, deduced as the difference between the sum energy and the α energy of ^{219}Pa, is 9477(44) keV.

The half-life of ^{223}Np was determined to be $2.15(^{100}_{52})$ μs by averaging the time differences between ^{223}Np implantations and decays, the errors were calculated following the method in Ref. [30]. The half-life of ^{223}Np is comparable to the time of flight (TOF) in SHANS. The influence of TOF on the half-life measurement in such situation has been analyzed and simulated in detail in [31], and was found negligible. The half-life of ^{219}Th was analyzed this way and was obtained as $1.06(^{7}_{6})$ μs, in agreement with the result of exponential fitting shown in Fig. 1.

Similarly, the half-life of ^{219}Pa was derived to be $60(^{28}_{15})$ ns by extracting the time differences between $\alpha(^{223}$Np) and $\alpha(^{219}$Pa) signals through the first derivative of the curve obtained from fitting the waveform (see the details in Supplemental Material). It is in agreement with the previous value of 53(10) ns obtained in [19]. The half-life of ^{215}Ac was obtained as $193(^{97}_{49})$ ms, consistent with the literature value of 170(10) ms [29] as well.

From the ^{175}Lu target data, a transport efficiency of 11(3)% was extracted for the ^{175}Lu(^{40}Ar, 4n/5n)^{211,210}Ac reaction channels,

Table 1

Decay chains attributed to the new isotope ^{223}Np. α_i represents α particle from ^{223}Np, ^{219}Pa, ^{215}Ac and ^{211}Fr, for $i = 1, 2, 3$ and 4, respectively. The units are keV for the implantation energy of ER, α particle energies and standard deviations (σ). The column ($E_{\alpha 1} + E_{\alpha 2}$) lists the sum energy of two overlapping α signals.

Event No.	E_{ER}	$E_{\alpha 1}$	σ_1	$E_{\alpha 2}$	σ_2	($E_{\alpha 1} + E_{\alpha 2}$)	σ_{sum}	$E_{\alpha 3}$	$E_{\alpha 4}$	$T_{\alpha 1}$/μs	$T_{\alpha 2}$/ns	$T_{\alpha 3}$/ms	$T_{\alpha 4}$/s
1	12891	9454	30	9992	30	19446	40	7596		4.58	239	6.8	
2	13940	9404[a]		10033[a]		19437	40	7593	862	1.88	43	142.7	8.2
3	9963	9568[a]		9879[a]		19447	40	1122	6536	4.28	80	141.2	210.4
4	14652	9316[a]		10133[a]		19449	40	7593		2.60	39	621.3	
5	10721					19484	40		6521	9.36	30		55.3
6	12935	752	60	9961	60	10713	40	7591		0.72	140	1023.0	
7	16375	2455	60	1016	60	3471	40	7586		1.20	160	194.0	
8	12079	1093[a]		9793[a]		10886	40	7584		1.74	19	231.9	
9	15260	1785[a]		10714[a]		12499	40	7599		0.30	44	131.3	
10	13181	9381[a]		731[a]		10112	40	7601		4.42	81	19.3	

[a] The α energies extracted from α(^{223}Np)–α(^{219}Pa) pileup pulses with time differences shorter than 100 ns cannot be reliably quantified.

similar to the value reported in [25] where the same reaction at beam energy of 177 MeV was used. Taking into account the time of flight in the SHANS spectrometer of around 1.3(1) μs and the detection efficiency of ∼50% for each generation α decay, the production cross-section of ^{223}Np at the mid-target energy ∼185 MeV was estimated to be $0.9\binom{3}{2}$ nb, comparable with the HIVAP prediction of 1.3 nb. The error of the measured cross-section represents the statistical error only.

3. Discussion

The spins and parities of the $N = 128$ and 130 isotones were all determined to be $9/2^-$ for odd-Z between 83 and 91 [29], including ^{219}Pa, the daughter nucleus of ^{223}Np, indicating that the odd-proton is filling the $\pi h_{9/2}$ orbital up to Pa. They decay to the ground states of their daughters and no fine structures were observed. Around $Z = 92$, the proton Fermi surface is closest to the $h_{9/2}$ and $f_{7/2}$ orbitals. The spin of ^{223}Np is expected to be different if a subshell closure exists at $Z = 92$, while not vice versa.

Based on the experimental systematics of low-lying levels in the odd-Z $N = 128$ isotones [29] and shell-model calculations presented below, the excitation energy of the first excited state $7/2^-$ in ^{219}Pa is expected to be around 350 keV and decay to the g.s. by γ transition. The internal conversion coefficient for such a transition is smaller than 0.6. Taking into account the detection efficiency of conversion electron within one pixel, the chance for the energy summing of α with conversion electron is negligible. So the measured charged-particle energy comes from α only.

If ^{223}Np has a $9/2^-$ ground state, as predicted by the shell-model calculations presented below, the α decay to the $9/2^-$ g.s. of ^{219}Pa is expected to be dominant, consistent with the fact that only one α line is observed. If ^{223}Np has a $7/2^-$ ($f_{7/2}$) ground state, the $7/2^- \rightarrow 9/2^-$ g.s. to g.s. transition is strongly hindered due to the spin flip between the initial and final states, it will decay to the $7/2^-$ excited state in ^{219}Pa with α energy 9477 keV, followed by γ transition.

Detailed information on nuclear structure can be obtained from the α-particle preformation probability inside the nucleus [32], which microscopically quantifies the stability against α decay. Conventionally, an equivalent variable, the reduced width for α decay δ^2 [33], which takes into account the angular momentum of the emitted α particle, is used. For the two possible α-decay paths above, where spins and parities of initial and final states are identical, the reduced decay width is calculated to be $0.17\binom{8}{4}$ MeV using the Q_α of 9687(45) keV and $T_{1/2}$ obtained for ^{223}Np in this work, comparable to those of neighboring $N = 130$ isotones with $Z = 86$–91 as shown in Fig. 3.

With the newly measured α-decay energy of ^{223}Np, single proton separation energies (S_p) can be extracted beyond $Z = 92$ along the $N = 130$ isotonic chain and are presented in Fig. 4. The S_p and
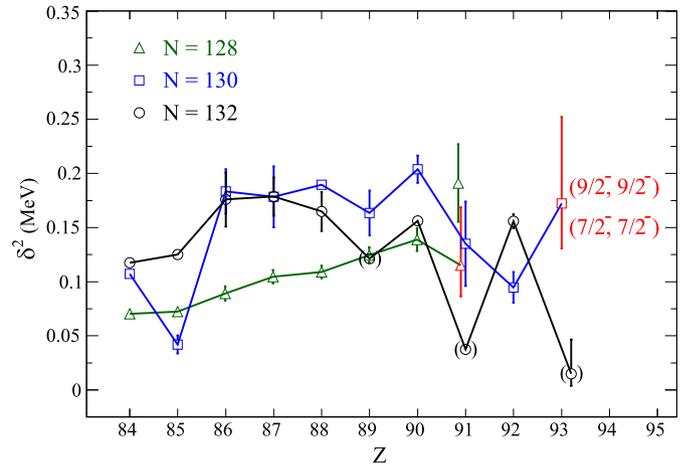
Fig. 3. The reduced α-decay widths of $N = 128$, 130 and 132 isotones as a function of Z. The reduced decay widths of ^{223}Np and ^{219}Pa obtained from the present work are plotted in red, while the value for ^{219}Pa extracted from the previous experimental results [19] is plotted in green. The reduced widths of ^{222,224}U were obtained using the latest experimental results from [14,34]. The data points of ^{221}Ac, ^{223}Pa and ^{225}Np are in parentheses as their J^π values are tentative. The J^π of ^{221}Ac was assigned tentatively as $(3/2^-)$ in [29]; The J^π of ^{223}Pa is assumed to be $(5/2^-)$ here, same as that of ^{227}Pa [29]; The J^π of ^{225}Np was assigned as $9/2^-$ from the systematic trend [29,35]. (Color online)

δ_p (separation energy difference) values for the two possible decay paths corresponding to $9/2^-$ or $7/2^-$ g.s. of ^{223}Np follow the trend before $Z = 92$, showing no sign of the subshell closure at $Z = 92$.

Large-scale shell-model calculations had been performed for the $N = 126$ isotones up to Pa ($Z = 91$) in the full $Z = 82$–126 proton model space $\pi(0h_{9/2}, 1f_{7/2}, 0i_{13/2}, 2p_{3/2}, 1f_{5/2}, 2p_{1/2})$ [6]. In order to understand the structure/spin-parity of ^{223}Np, similar calculations but in a truncated space are performed for the $N = 130$ and 128 isotones in this region. The calculations are performed with Hamiltonian KHPE [37] using the code KSHELL [38]. KHPE is a modification on Kuo–Herling interaction [39] and gives nice description on nuclei with $Z > 82$ and $N > 126$ [7,6,40,41]. The model space for KHPE is $\pi(0h_{9/2}, 1f_{7/2}, 1f_{5/2}, 2p_{3/2}, 2p_{1/2}, 0i_{13/2})$ and $\nu(0i_{11/2}, 1g_{9/2}, 1g_{7/2}, 2d_{5/2}, 2d_{3/2}, 3s_{1/2}, 0j_{15/2})$. The full model space calculations for ^{219}Pa and ^{223}Np are beyond the computational limit because of the large total number of valence protons and neutrons. A truncated model space $\pi(0h_{9/2}, 1f_{7/2}, 0i_{13/2})\nu(0i_{11/2}, 1g_{9/2}, 0j_{15/2})$ is used. Further restrictions on the model space are made in two ways: one is that the maximum occupancy numbers in each of the $\pi 1f_{7/2}, \pi 0i_{13/2}, \nu 0i_{11/2}, \nu 0j_{15/2}$ orbitals are two protons or neutrons; the other is that the maximum occupancy number in $\pi 0i_{13/2}$ orbital is four protons while those in other orbitals are still two. The latter restriction on ^{223}Np reaches
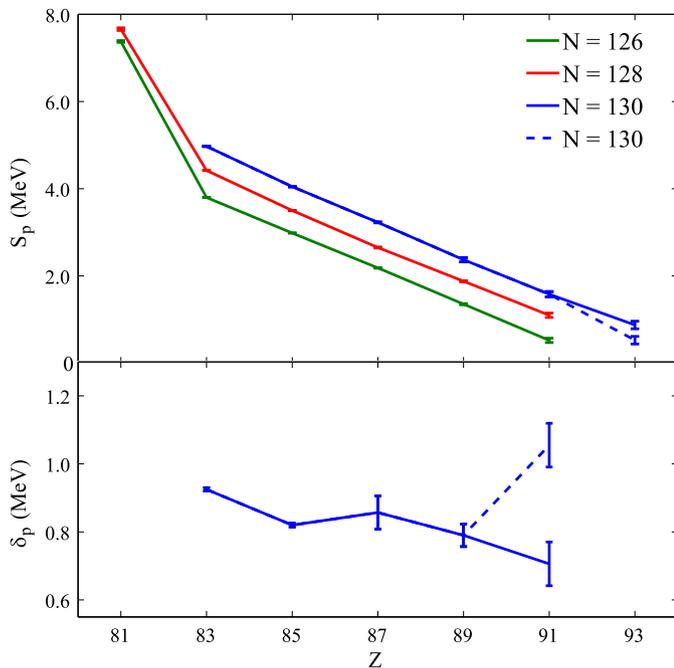
Fig. 4. Proton separation energies of $N = 126$, 128 and 130 isotones of odd-Z Tl-Np (upper panel) and the separation energy differences δ_p for $N = 130$ isotones (lower panel). The binding energies of ^{223}Np and ^{219}Pa are obtained from the α-decay data of this work, ^{222}U from [14] and the others from [36]. The S_p and δ_p values related with the $9/2^-$ g.s. of ^{223}Np are guided with straight lines, while those with the $7/2^-$ g.s. are guided with dashed lines. (Color online)

the computational limit of shell-model calculations, $\sim 10^{10}$ dimensions.

The spins and parities of the first few states obtained for the $N = 126$ isotones using such truncated model spaces are found to be the same with those obtained using the full model space in [6], giving us confidence in the present calculations in the truncated model space. The spins and parities of ^{223}Np and ^{219}Pa are calculated to be both $9/2^-$. In the previous shell-model calculations [6], the ground state of the semi-magic ^{219}Np was predicted to be $9/2^-$ as well.

Based on the large-scale shell-model calculations above, spin and parity of $9/2^-$ are tentatively proposed for the ground state of ^{223}Np, supporting the absence of a subshell closure at $Z = 92$ and $N = 130$. However, an α–γ coincidence experiment with much higher statistics than in the present work is needed to exclude/confirm the alternative $7/2^-$ spin and parity.

It should be noted however that the reduced decay width of ^{222}U is anomalously small compared with those of other $N = 130$ isotones, even smaller than those of the neighboring odd-Z ^{221}Pa and ^{223}Np. As the present results for ^{223}Np and the previous data for $N = 126$ isotones do not support the existence of a $Z = 92$ subshell closure around $N = 126$, the reason remains unclear and this anomaly calls for further study.

4. Summary

In summary, we report on the discovery of the new short-lived isotope ^{223}Np, which was synthesized in the fusion reaction ^{40}Ar $+$ ^{187}Re and identified through temporal and spatial correlations with subsequent α decays in the decay chain starting from ^{223}Np. The half-life and energy were extracted to be $T_{1/2} = 2.15\binom{100}{52}$ μs and $E_\alpha = 9477(44)$ keV from pileup traces by using modern digital pulse processing techniques. The energy of individual α in pileup trace with time difference between overlapping signals down to

$\sim$100 ns was extracted, the shortest analyzed so far using this method. The trend in proton separation energy shows no sign of a $Z = 92$ subshell closure. The spin and parity of ^{223}Np are proposed to be $9/2^-$ by combining the reduced α-decay width and large-scale shell-model calculations in truncated model space, negating the presence of a $h_{9/2}$ subshell closure at $Z = 92$ near $N = 126$. The decay chain of ^{219}Pa, the shortest-lived α emitter known with directly measured half-life, was established for the first time.

Appendix A. Supplementary material

Supplementary material related to this article can be found online at http://dx.doi.org/10.1016/j.physletb.2017.03.074.

References

[1] K.N. Rutz, M. Bender, P.-G. Reinhard, J.A. Maruhn, W. Greiner, Nucl. Phys. A 634 (1998) 67.
[2] L.S. Geng, H. Toki, J. Meng, Prog. Theor. Phys. 113 (2005) 785.
[3] L.S. Geng, J. Meng, H. Toki, W.-H. Long, G. Shen, Chin. Phys. Lett. 23 (2006) 1139.
[4] H. Sagawa, G. Colo, Prog. Part. Nucl. Phys. 76 (2014) 76.
[5] P. Möller, J.R. Nix, K.-L. Kratz, At. Data Nucl. Data Tables 66 (1997) 131.
[6] E. Caurier, M. Rejmund, H. Grawe, Phys. Rev. C 67 (2003) 054310.
[7] K. Hauschild, et al., Phys. Rev. Lett. 87 (2001) 072501.
[8] A.P. Leppänen, et al., Phys. Rev. C 75 (2007) 054307.
[9] A. Astier, M.-G. Porquet, Phys. Rev. C 87 (2013) 014309.
[10] J. Rissanen, et al., Phys. Rev. C 90 (2014) 044324.
[11] W.H. Long, H. Sagawa, N. Van Giai, J. Meng, Phys. Rev. C 76 (2007) 034314.
[12] W.H. Long, T. Nakatsukasa, H. Sagawa, J. Meng, H. Nakada, Y. Zhang, Phys. Lett. B 680 (2009) 428.
[13] W.H. Long, P. Ring, J. Meng, N. Van Giai, C.A. Bertulani, Phys. Rev. C 81 (2010) 031302(R).
[14] J. Khuyagbaatar, et al., Phys. Rev. Lett. 115 (2015) 242502.
[15] G. Gamow, Z. Phys. 51 (1928) 204.
[16] R.G. Thomas, Prog. Theor. Phys. 12 (1954) 253.
[17] A.N. Andreyev, et al., Phys. Rev. Lett. 110 (2013) 242502.
[18] S.N. Liddick, et al., Phys. Rev. Lett. 97 (2006) 082501.
[19] T. Faestermann, A. Gillitzer, K. Hartel, W. Henning, P. Kienle, in: Proc. 5th Int. Conf. Nuclei Far from Stability, Rosseau Lake, Canada, K12, 1987.
[20] K. Nishio, H. Ikezoe, S. Mitsuoka, J. Lu, Phys. Rev. C 62 (2000) 014602.
[21] H.M. Devaraja, et al., Phys. Lett. B 748 (2015) 199.
[22] A.V. Yeremin, et al., Nucl. Instrum. Methods Phys. Res., Sect. A 350 (1994) 608.
[23] R. Grzywacz, Nucl. Instrum. Methods Phys. Res., Sect. B 204 (2003) 649.
[24] W. Reisdorf, Z. Phys. A 300 (1981) 227.
[25] Z.Y. Zhang, et al., Nucl. Instrum. Methods Phys. Res., Sect. B 317 (2013) 315.
[26] D. Kaji, K. Morita, K. Morimoto, H. Haba, H. Kudo, Proc. Radiochim. Acta 1 (2011) 105.
[27] http://www.caen.it/csite, 2016 (accessed 15 September 2016).
[28] V.T. Jordanov, G.F. Knoll, Nucl. Instrum. Methods Phys. Res., Sect. A 345 (1994) 337.
[29] http://www.nndc.bnl.gov/ensdf/, 2016 (accessed 09 October 2016).
[30] K.-H. Schmidt, et al., Z. Phys. A 316 (1984) 19.
[31] X.Y. Liu, et al., to be published.
[32] H.J. Mang, Annu. Rev. Nucl. Sci. 14 (1964) 1.

[33] J.O. Rasmussen, Phys. Rev. 113 (1959) 1593.
[34] A. Lopez-Martens, et al., Eur. Phys. J. A 50 (2014) 132.
[35] G. Audi, et al., Chin. Phys. C 36 (2012) 1157.
[36] M. Wang, et al., Chin. Phys. C 36 (2012) 1603.
[37] E.K. Warburton, B.A. Brown, Phys. Rev. C 43 (1991) 602.

[38] N. Shimizu, arXiv:1310.5431, 2013.
[39] T.T.S. Kuo, G. Herling, U.S. Naval Research Laboratory Report No. 2258, 1971;
G. Herling, T.T.S. Kuo, Nucl. Phys. A 181 (1972) 113.
[40] A.I. Morales, et al., Phys. Rev. C 89 (2014) 014324.
[41] N. Cieplicka-Oryńczak, et al., Phys. Rev. C 93 (2016) 054302.